Characterization of the Surface Morphology of Durum Wheat Starch Granules Using Atomic Force Microscopy

S. NEETHIRAJAN,[1] D.J. THOMSON,[2] D.S. JAYAS,[1]* AND N.D.G. WHITE[3]
[1]*The Canadian Wheat Board Centre for Grain Storage Research, Department of Biosystems Engineering, University of Manitoba, Winnipeg, MB R3T 5V6, Canada*
[2]*Department of Electrical and Computer Engineering, University of Manitoba, Winnipeg, MB R3T 5V6, Canada*
[3]*Agriculture and Agri-Food Canada, Cereal Research Centre, Winnipeg, MB R3T 2M9, Canada*

KEY WORDS AFM; growth rings; wheat starch; vitreous; nonvitreous

ABSTRACT Knowledge of the structure and properties of microscopic surfaces of durum wheat starch granules is essential for understanding the functional and physico-chemical properties. The nanoscale surface undulations on the starch granules inside durum wheat macroscopically influence the milling properties. The objective of this study was to visualize the surface morphology and the size of starch grains of vitreous and nonvitreous durum wheat kernels using atomic force microscopy. The distribution of starch granules in the vitreous and nonvitreous durum wheat starch samples were examined and compared. The results of our study confirm the 'blocklet' model of the ultrastructure of the starch granule surface. Image contrast enhancement using UV/ozone treatment of microtomed starch samples improved the imaging of growth rings on the starch samples. The observation of growth rings in the nonvitreous starch granule surfaces indicates that amylopectin is more common than amylose in nonvitreous starch when compared with vitreous starch. *Microsc. Res. Tech. 71:125–132, 2008.*

INTRODUCTION

The annual world production of durum wheat is about 26 Mt (million tons) (USDA, 2005). Durum wheat is used for making semolina and pasta. One of the important factors in determining the quality of durum wheat is vitreousness. Vitreous durum wheat kernels are glassy and translucent in appearance while nonvitreous kernels contain a more opaque starchy or mottled appearance (Fig. 1). There are strict tolerances for the number of nonvitreous kernels allowed into durum grades during export.

Vitreousness of durum kernels is associated with semolina granulation, color, and protein content. The less vitreous the kernels, the finer the granulation and lower the color and protein content. Less vitreous kernels produce more flour thus resulting in less semolina product. Generally, vitreous kernels are harder than nonvitreous kernels (Dexter et al., 1989). Wheat flour from soft kernels has higher water absorption capacity resulting in more bread from a given weight of flour (Dexter and Marchylo, 1996). Hard wheat has vitreous endosperm which offers higher resistance to milling than the nonvitreous soft wheat.

The size and distribution of starch granules play a role in understanding functional and physico-chemical properties. Starch granule size distribution and the total volume occupied by starch granules affect the elastic modulus and mixing time of dough and thereby, the rheological properties of wheat flour. Increased proportions of smaller size granules increase the dough's elastic character (Edwards et al., 2002). Morphology and topography of a surface is also an important feature of solids used as raw material (Aguilera, 2000). The surface of the starch granule determines the granule hydration and the vulnerability to enzyme attack, and affects chemical reactions with modifying agents during milling and processing of wheat flour (Banks and Greenwood, 1975). The nanoscale nature of the surface undulations on the starch granules from durum wheat is relevant since it influences the wheat's milling and functional properties. Measurement of the size and observation of the surface of starch granules can help us understand the difference in functional properties of vitreous and nonvitreous kernels.

Atomic Force Microscopy (AFM) is a powerful technique that makes it possible to analyze surface features down to the molecular level. Employment of AFM in food and cereal science research is occurring at a rapid pace. Morris et al. (2001) have proven that AFM is an excellent tool for interpreting rheology of food biopolymers. AFM has been used to image the starch granule surfaces of barley, oat, corn, and maize (Baker et al., 2001; Juszczak et al., 2003; Ohtani et al., 2000). AFM has also been used to image bacteria of different taxonomy groups (Bolshakova et al., 2004) and the roughness of the skin of peaches during controlled atmosphere storage (Yang et al., 2004).

*Correspondence to: D.S. Jayas, The Canadian Wheat Board Centre for Grain Storage Research, Department of Biosystems Engineering, University of Manitoba, Winnipeg, MB R3T 5V6, Canada. E-mail: digvir_jayas@umanitoba.ca

Received 6 May 2007; accepted in revised form 4 September 2007

Contract grant sponsors: Canada Research Chairs Program, Canada Foundation for Innovation, Manitoba Research Innovation Fund, University of Manitoba, Natural Sciences and Engineering Research Council of Canada.

DOI 10.1002/jemt.20534

Published online 15 October 2007 in Wiley InterScience (www.interscience.wiley.com).

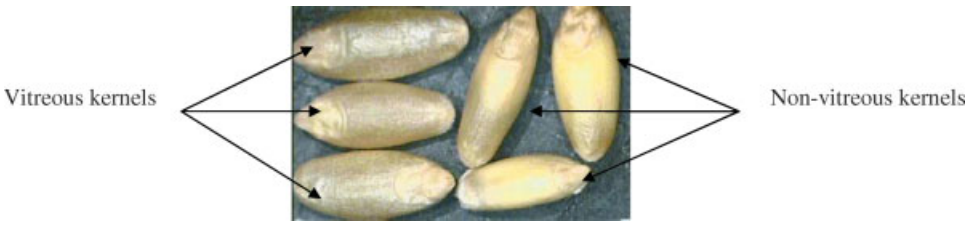

Fig. 1. Photographic image of vitreous and nonvitreous durum wheat kernels.

Surface investigation and material characterization could have been done by scanning electron microscopy (SEM); however, one major drawback of SEM is that it requires the samples to be dried and coated with metals. The poorly conducting starch granule surface requires a conductive coating or staining to prevent charging. In our study, metal coating cannot be done on the starch samples as it will damage the granule surfaces. Coatings may also alter or obscure the granule surface features resulting in the loss of information or create artifacts. Environmental SEM methods require low-voltage operation in a environmental chamber which will sacrifice image resolution.

The AFM technique is nondestructive and does not rely on the sample being electrically conductive. Scanning of samples is conducted in air or in liquid unlike the SEM which needs a vacuum for the sample. Unlike SEM, AFM can measure surface structure in all three dimensions with a single scan making it possible to estimate surface roughness and its surface variation. AFM also provides height information with good vertical resolution.

The working principle of AFM is presented in depth in several books and articles (Binnig et al., 1986; Dufrene, 2001; Morris et al., 1999; Yang and Shao, 1995). For biosystems engineers and biologists, AFM offers the prospect of making high-resolution images of biological material (images of molecules and their interactions under physiological conditions, and the study of molecular processes in living systems). The preparation of samples for AFM imaging is challenging and considerable research has been devoted to this topic. In this article, we present work that demonstrates the use of ozone to image the internal structure of a wheat starch granule.

The objectives of this study were (1) to visualize the size and surface morphology of the starch granules of vitreous and nonvitreous durum wheat using AFM and (2) to characterize the starch granule surface differences of vitreous and nonvitreous durum kernels.

MATERIALS AND METHODS

Samples

Durum wheat (*Triticum turgidum* L.) sample of 10 kg was collected from a terminal elevator at Thunder Bay, Canada (Fig. 1). In Canada, all cultivars of same class of wheat (e.g. durum), grown in different regions, are mixed at the terminal elevator. The single sample thus represents a composite sample of a particular class. Two subsamples of 1 kg each for vitreous and nonvitreous types were manually separated from the 10-kg sample by visual assessment. Other than avoiding the weathered and bleached kernels in the subsamples, the subsamples were separated randomly. Starch samples from the vitreous and the nonvitreous subsamples were prepared using the following steps: (1) dough preparation, (2) dough tempering, (3) elution of starch using 0.1% aqueous NaCl solution, (4) centrifugation of starch suspension, (5) elimination of supernatant and impurities, (6) starch drying (freeze drying), (7) starch lumps disintegration, and (8) starch sieving (0.09 mm). Starch prepared from both the vitreous and nonvitreous subsamples was collected separately in two different plastic bags. Dough preparation involves (i) cleaning the wheat from chaff and foreign material and (ii) grinding the wheat kernels using a BRABENDER mill (Brabender Gmbh, Germany). Tempering optimizes the moisture content and makes the dough less liable to starch damage. Dough tempering was done at 30°C for 60 min in the dough tempering bin.

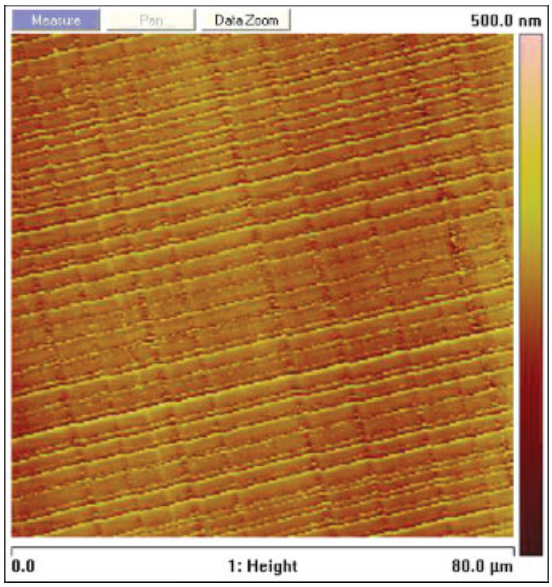

Fig. 2. AFM images of pure Spurr's resin samples. Scan size areas of the images are (a) $(80\ \mu m)^2$ and (b) $(10\ \mu m)^2$.

Sectioning Using a Microtome

AFM imaging should be done on a flat surface to avoid large height differences and to prevent tip imaging artifacts. Starch granules placed on a slide might be swept away or break apart due to probe movement in the contact mode during scanning. Hence, embedding the starch granules in a resin was necessary. A

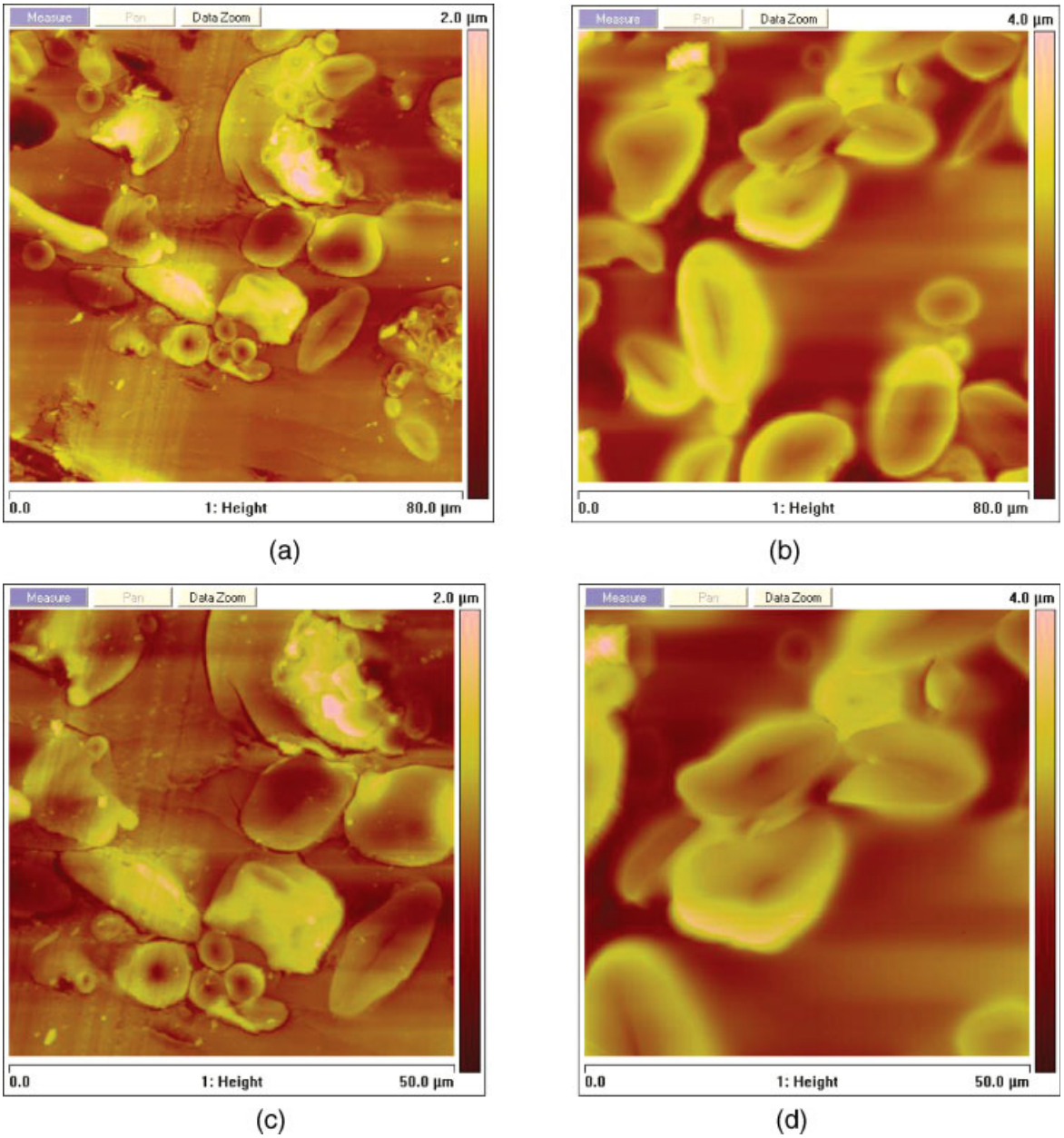

Fig. 3. AFM images of durum wheat starch granule surfaces before UV/ozone treatment. (**a**, **c**) are vitreous starch granules and (**b**, **d**) are nonvitreous starch granule images. The scan size areas are $(80\ \mu m)^2$ for images (a, b) and $(50\ \mu m)^2$ for images (c, d). [Color figure can be viewed in the online issue, which is available at www.interscience.wiley.com.]

small quantity of starch granules (6.3 mg) was placed in the bottom of a plastic BEEM capsule and embedded in fresh Spurr's epoxy resin. Fresh Spurr's for embedding is composed of four different components namely (i) 10.0 g of ERL 4206 (vinyl cyclohexane dioxide), (ii) 6.0 g of DER 736 (diglycidyl ether of propylene oxide), (iii) 26 g of NSA (neonyl succinic anhydride), and (iv) 0.4 g of DMAE (dimethylaminoethanol).

Using a pointed wooden needle, the starch sample was lightly stirred to help any air bubbles to escape. After 15 min of settling, the BEEM capsule was polymerized in an oven at 70°C for 12 h. The sample was carefully removed from the capsule and placed directly into the microtome chuck. The block face was polished using a Reichert-Jung Ultracut microtome (Leica Microsystems, Wetzlar, Germany). A smoothness of less than 0.5 µm was achieved at the exposed surface of the resin using a fresh dry glass knife. Once the block face was cut, the block was removed and the sample was ready for imaging. Five samples of both the vitreous and nonvitreous starch samples were embedded in resin and prepared in similar fashion. Two sample BEEMs were also prepared with only the Spurr's epoxy resin for reference imaging.

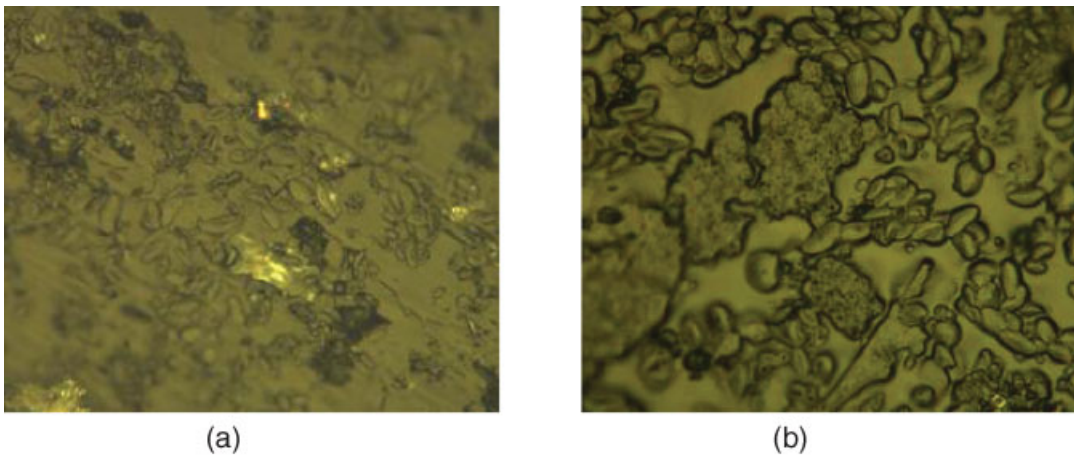

Fig. 4. Optical microscope images of exposed starch granule surfaces embedded in Spurr's epoxy resin. Scan size area is (3 mm)^2 (**a**) vitreous kernel starch granules, (**b**) nonvitreous kernel starch granules. [Color figure can be viewed in the online issue, which is available at www.interscience.wiley.com.]

Contrast Enhancement

The starch samples embedded in the epoxy resin were subjected to UV/ozone treatment to enhance the ability to see certain structures in the image. UV/ozone treatment has an effect on surface characteristics by decreasing the surface roughness of organic polymers (Viallet et al., 2003). The UV/ozone treatment was performed using a commercial system (UVO-Cleaner Model 144A, Jelight Company, Irvine, CA) with a low-pressure mercury vapor grid lamp as the UV source. The starch samples were subjected to UV/ozone treatment for 30 s, 1 min, 2 min, and then imaged with AFM within 20 min. An appropriate optimization of plasma etching provided a controlled modification of the surface topography of polymer surfaces (Tserepi et al., 2003). Hence, the starch samples embedded in the Spurr's resin were subjected to plasma etching for 30 s, 1 min, and 2 min. The plasma etching was performed using a Trion ICP plasma etcher (Trion Technology, Clearwater, FL). The plasma etched samples were imaged using AFM immediately after etching.

Imaging

A Dimension 3100 AFM (Digital Instruments, Santa Barbara, CA) and an Olympus BX51 optical microscope (Olympus Optical Company, Tokyo, Japan) were used to image the samples. A 12V/100W halogen illumination source was used with the optical microscope for the bright field imaging of the embedded starch samples. The AFM imaging was performed in the contact mode with a silicon nitride probe mounted on a cantilever with a normal spring constant of 0.06–0.12 N/m. Scan areas varied between 100 μm × 100 μm and 1 μm × 1 μm. A total of 12 samples (5 vitreous and 5 nonvitreous and 2 reference resins) were scanned using the AFM.

RESULTS AND DISCUSSION

An AFM image is a combination of the surface morphology and the shape of the AFM tip. Localized interaction between the tip and the starch surface may create artifacts, resulting in distorted images, uncharacteristic of the actual sample. It is necessary to ensure that the image scanned truly reflects the surface features of the sample rather than representing a tip artifact. A typical reference image of a plastic BEEM capsule containing only the microtomed resin is shown in Figure 2. The knife marks are visible on the surface of the resin, which did not adversely affect AFM imaging. Figure 3 shows the AFM images of vitreous and nonvitreous durum granules for one of the samples before UV/ozone treatment at different scan area sizes. For the other four samples, similar images were obtained; therefore, images from only one representative sample are shown. A comparison of the images in

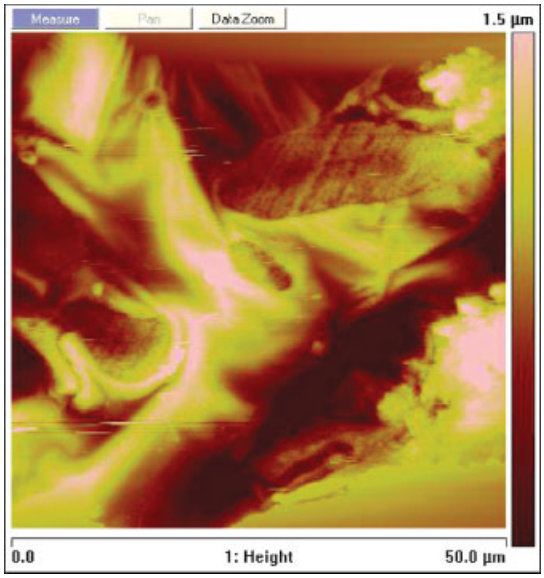

Fig. 5. AFM image of durum wheat vitreous starch granule surfaces after UV/ozone treatment for 30 S for a (50 μm)^2 scan area. [Color figure can be viewed in the online issue, which is available at www.interscience.wiley.com.]

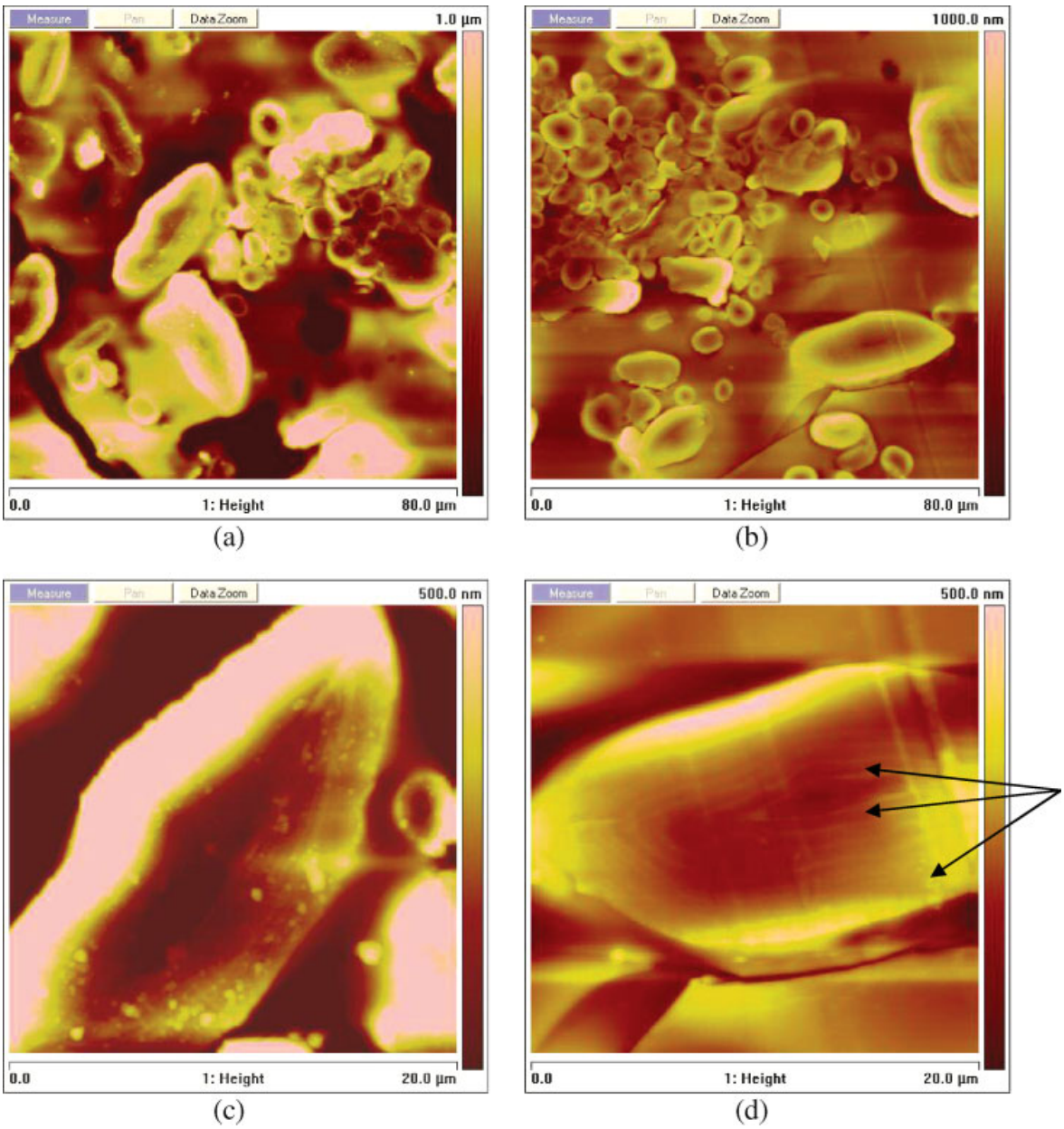

Fig. 6. AFM images of durum wheat starch granule surfaces after UV/ozone treatment. (**a**, **c**) are vitreous starch granules and (**b**, **d**) are nonvitreous starch granule images. The scan size areas are (80 µm)^2 for images (a, b) and (20 µm)^2 for images (c, d). Arrows in (d) indicates visible growth ring pattern on the starch granule surface. [Color figure can be viewed in the online issue, which is available at www.interscience.wiley.com.]

Figures 2 and 3 shows that the granules observed in the Figure 3 are starch grains and can be easily distinguished from sectioning artifacts. The starch granules are easily distinguishable from the resin and also from the knife marks created during sectioning. The surface smoothness was ~0.5 µm and care was taken to ensure that individual starch granules were not cleaved during sectioning in the microtome. There was no infiltration of resin into the starch granules and this lack of infiltration was verified by examination of the embedded starch samples with the optical microscope because there is a difference in contrast between the starch granules and the encasing resin (Fig. 4). Nonvitreous starch granules are larger in size than vitreous starch granules and the starch granules were not cleaved internally (Fig. 4).

Plasma etching of starch samples for 30 s or more, damaged the starch sample surfaces (Fig. 5). Plasma etching did not enhance starch surface topography. The use of plasma etching for surface coating removal is practical only for a coating which has uniform thickness but will not work for biological materials such as wheat starch (Shaw et al., 2000). As the plasma process etches the surface from all areas at roughly the same

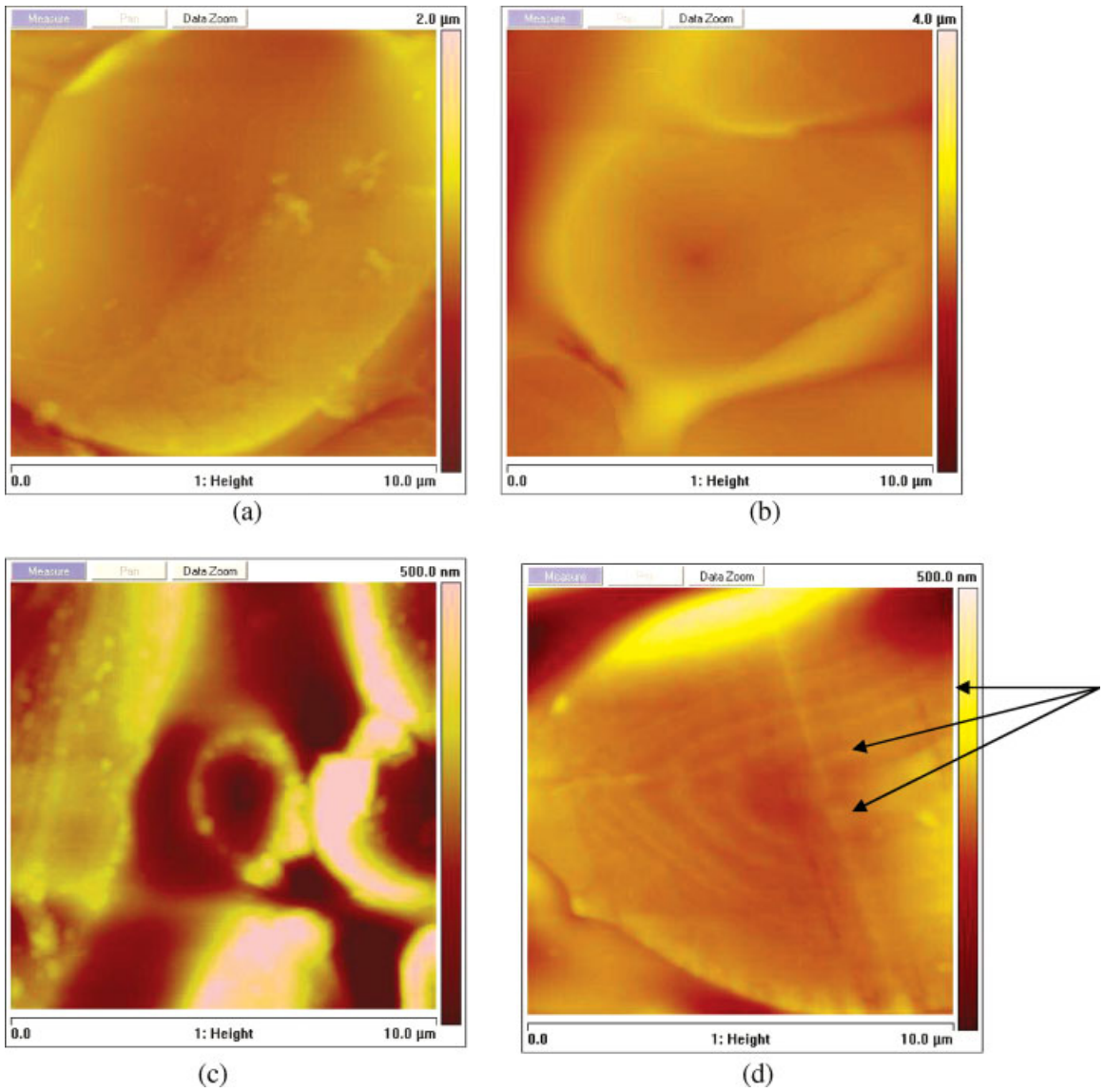

Fig. 7. AFM images of durum wheat starch granule surfaces. The scan size areas are $(10\ \mu m)^2$. (**a**, **b**) are vitreous and nonvitreous starch images obtained before UV/ozone treatment. (**c**, **d**) are vitreous and nonvitreous starch images obtained after UV/ozone treatment. Arrows in (d) indicates visible growth ring pattern on the starch granule surface. [Color figure can be viewed in the online issue, which is available at www.interscience.wiley.com.]

rate, the nonuniformity in the surface topography may have resulted from damage to the starch granule surface.

The starch granules subjected to UV/ozone treatment for 1 min provided better images in comparison with 30 s and 2 min exposure to UV/ozone. Two minutes of UV/ozone exposure greatly decomposed the starch granules due to over oxidation of the surfaces. There was no visible difference between the untreated and the 30 s UV/ozone treated starch granule samples. Hence, the starch granule samples treated for 1 min were used in this study.

Granule Analysis

The surfaces of starch granules appeared smooth with few nodules and depressions. The surfaces of 78 vitreous starch granules and 80 nonvitreous starch granules were examined. Starch granules with diameters ranging from 10 to 50 nm and ranging from 50 to 350 nm were found in both the vitreous and nonvitreous kernels. A greater number of larger diameter starch granules were found in the nonvitreous starch granule samples compared to the vitreous granules.

Growth Rings

The AFM images of the UV/ozone treated starch samples improve their surface images over the non-treated sample images (Fig. 6). This is believed to arise from a difference in the rate at which the ozone etches the various components of the starch granules. Growth rings are observed at a 20 µm × 20 µm scan area of the

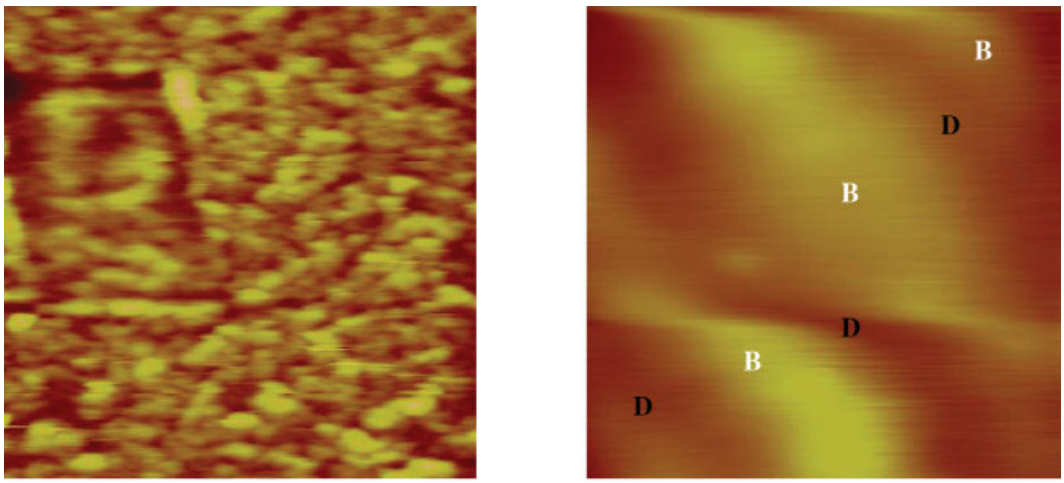

Fig. 8. AFM images of durum wheat starch granule surfaces after UV/ozone treatment. (**a**, **b**) are vitreous and nonvitreous starch granules at $(3\ \mu m)^2$ scan size area. B and D on the nonvitreous image indicate bright and dark banding patterns of starch. [Color figure can be viewed in the online issue, which is available at www.interscience.wiley.com.]

nonvitreous starch samples (Fig. 6d) after UV/ozone treatment but growth rings are not visible in the untreated starch samples. The topographic images of the nonvitreous starch granule after UV/ozone treatment (Fig. 7d) clearly show the growth rings which are not present in the vitreous starch granule surfaces. Vitreousness in wheat kernels are caused by genetic factors (Symes, 1969) and biochemical factors (Simmonds, 1978). The degree, to which wheat becomes nonvitreous, is also decided by weather conditions (Phillips and Niernberger, 1976). The distribution of the amylopectin unit-chains in starch is genetically controlled and is characteristic of a species (Kalichevsky et al., 1990).

Basically starch consists of two types of molecules, amylose and amylopectin. The relative proportion of amylose to amylopectin depends on the source of the starch (Singh et al., 2003). Amylopectin molecules of the starch generate concentric layers that contribute to the growth rings of the starch (Parker and Ring, 2001). Nonvitreous kernels have lower amylose content than vitreous kernels (El-Khayat et al., 2003). Our observation of growth rings explains that nonvitreous kernels have more amylopectin than amylose.

Ultra Structure of Granules

The Blocklet model describes the organization of a starch granule and its architecture. Repeating crystalline and amorphous lamellae interspaced by growth rings on the inner starch granule surfaces is the blocklet concept. The amylopectin molecules are radially arranged with their axes perpendicular to the starch granule surface and to the growth rings (Gallant et al., 1997). In Figure 8, the embedding of crystalline units has occured in amorphous material of the granule surface. Inspection of the banding pattern observed in the samples at higher resolution (Fig. 8), reveals that the dark bands are sometimes discontinuous. Bright and dark banded blocklet structures are clearly visible in Figure 8b. This is consistent with the blocklet model proposed in a previous study (Ridout et al., 2002). The banding pattern is not clearly distinguished in vitreous starch.

CONCLUSIONS

The AFM, combined with ozone contrast enhancement, is a powerful tool to study the ultrastructure of starch granules. Our study confirms the 'blocklet model' of the ultrastructure of starch granule surface from nonvitreous kernels. Starch granules were larger in size and in higher number for nonvitreous granules compared to the vitreous granules. Growth rings were observed only in the nonvitreous starch granules. The nonvitreous durum wheat starch has more amylopectin molecules than amylose. Plasma etching did not assist in enhancing the surface topography of starch granule surface for AFM imaging. UV/ozone cleaning enhanced the imaging of the starch granule surface by clearly showing the growth rings. Our study demonstrates that AFM can be used by plant scientists to characterize the effects of genetics, growing conditions, and other biochemical factors on starch granules and thus develop cultivars which are more vitreous.

ACKNOWLEDGMENTS

The authors thank the Industry Services Division of the Canadian Grain Commission for providing durum wheat samples. The authors thank the technicians Jerry Suchy, Agriculture and Agri-Food Canada, Winnipeg and Dwayne Chrusch, Department of Electrical and Computer Engineering, University of Manitoba for their help in sample preparation and imaging.

REFERENCES

Aguilera JM. 2000. Microstructure and food product engineering. Food Technol 54:56–65.

Baker AA, Miles MJ, Helbert W. 2001. Internal structure of the starch granule revealed by AFM. Carbohydr Res 330:249–256.

Banks W, Greenwood CT. 1975. Starch and its components. Edinburgh, UK: Edinburgh University Press.
Binnig G, Quate CF, Gerber CH. 1986. Atomic force microscope. Phy Rev Lett 56:930–933.
Bolshakova A, Kiselyova O, Yaminsky IV. 2004. Microbial surfaces investigated using atomic force microscopy. Biotechnol Prog 20:1615–1622.
Dexter JE, Marchylo BA. 1996. Meeting the durum wheat quality requirements of an evolving processing industry: Past, present and future trends. Paper presented at the Pavan Mapimpianti 50th anniversary durum wheat and pasta seminars, Bassano del Grappa, Italy.
Dexter JE, Marchylo BA, MacGregor AW, Tkachuk R. 1989. The structure and protein composition of vitreous, piebald and starchy durum wheat kernels. J Cereal Sci 10:19–32.
Dufrene YF. 2001. Application of atomic force microscopy to microbial surfaces: From reconstituted cell surface layers to living cells. Micron 32:153–165.
Edwards NM, Dexter JE, Scanlon MG. 2002. Starch participation in durum dough linear viscoelastic properties. Cereal Chem 79:850–856.
El-Khayat GH, Samaan J, Brennan CS. 2003. Evaluation of vitreous and starchy syrian durum (*Triticum Durum*) wheat grains: The effect of amylose content on starch characteristics and flour pasting properties. Starch/Starke 55:358–365.
Gallant DJ, Bouchet B, Baldwin PM. 1997. Microscopy of starch: Evidence of a new level of granule organization. Carbohydr Polym 32:177–191.
Juszczak L, Fortuna T, Krok F. 2003. Non-contact atomic force microscopy of starch granules surface, Part 2: Selected cereal starches. Starch/Starke 55:8–18.
Kalichevsky MT, Orford PD, Ring SG. 1990. The retrogradation and gelation of amylopectins from various botanical sources. Carbohydr Res 198:49–55.
Morris VJ, Gunning AP, Kirby AR. 1999. Atomic force microscopy for biologists. London: Imperial College Press. 350 p.
Morris VJ, Mackie AR, Wilde AR, Kirby PJ, Mills AR, Gunning AP. 2001. Atomic force microscopy as a tool for interpreting the rheology of food biopolymers at the molecular level. Food Sci Technol 34:3–10.
Ohtani T, Yoshino T, Hagiwara S, Maekawa T, Tsukuba T. 2000. High resolution imaging of starch granule structure using atomic force microscopy. Starch/Starke 5:150–153.
Parker R, Ring SG. 2001. Aspects of the physical chemistry of starch. J Cereal Sci 34:1–17.
Phillips DP, Niernberger FF. 1976. Milling and baking quality of yellow berry and dark, hard and vitreous wheats. Bakers Dig 50:42–48.
Ridout MJ, Gunning AP, Wilson RH, Parker ML, Morris VJ. 2002. Using AFM to image the internal structure of starch granules. Carbohydr Polym 50:123–132.
Shaw H, Parekh N, Clatterbuck C, Frades F. 2000. Evaluation of ESD effects during removal of conformal coatings using micro abrasive blasting. Technology Validation Assurance Report. NASA Stennis Space Center, St. Louis, MS: NASA Official Press.
Simmonds DH. 1978. Structure, composition and biochemistry of cereal grains. In: Pomeranz Y, editor. Cereals '78: Better Nutrition for the World's Millions. St. Paul: American Association of Cereal Chemists. p. 105.
Singh N, Singh J, Kaur L, Sodhi NS, Gill BS. 2003. Morphological, thermal and rheological properties of starches from different botanical sources. Food Chem 81:219–231.
Symes KJ. 1969. Influence of a gene causing hardness on the milling and baking qualities of two wheats. Aust J Agric Res 20:971–979.
Tserepi A, Gogolides E, Constantoudis V, Cordoyiannis G, Raptis I, Valamontes ES. 2003. Surface roughness induced by plasma etching of Si-containing polymers. J Adhes Sci Technol 17:1083–1091.
USDA. 2005. Production estimates and crop assessment division. Washington, DC: United States Department of Agriculture.
Viallet B, Daran E, Malaquin L. 2003. Effects of ultraviolet/ozone treatment on benzocyclobutene films. J Vac Sci Technol A 21:766–771.
Yang J, Shao Z. 1995. Recent advances in biological atomic force microscopy. Micron 26:35–49.
Yang H, Feng G, Li Y. 2004. Investigating the roughness of peach during controlled atmosphere storage by atomic force microscopy. ASAE Paper No. 046186. St. Joseph, MI: ASAE.